Jurnal ELTIKOM :
Jurnal Teknik Elektro, Teknologi Informasi dan Komputer

Vol. 9, No. 1, June 2025, page. 78-90
ISSN 2598-3245 (Print), ISSN 2598-3288 (Online)
DOI: http://doi.org/10.31961/eltikom.v9i1.1489
Available online at http://eltikom.poliban.ac.id

DESIGN AND PERFORMANCE EVALUATION OF A PORTABLE LOW-HEAD PICO-HYDRO SYSTEM USING A REWOUND AXIAL GENERATOR FOR RURAL ENERGY

Aripriharta[1*], Ahmad Dhaffa Nibrosoma[1], Arif Nur Afandi[1], Mohamad Rodhi Faiz Nur Aini Syafrina Rahmadhani[1], Muhammad Cahyo Bagaskoro[1], Norzanah Rosmin[2]
[1)] Department of Electrical and Informatic Engineering, Universitas Negeri Malang, Malang, Indonesia
[2)]Department of Electrical Power Engineering, Faculty of Electrical Engineering, Universiti Teknologi Malaysia, Johor, Malaysia
e-mail: aripriharta.ft@um.ac.id, ahmad.dhaffa.2005366@students.um.ac.id, an.afandi@um.ac.id, mohamad.rodhi.ft@um.ac.id, nur.aini.2205366@students.um.ac.id, muhammad.cahyo.2305348@students.um.ac.id, norzanah@utm.my

Received: 19 March 2025 – Revised: 24 May 2025 – Accepted: 28 May 2025

ABSTRACT

This study evaluates the performance of a pico-hydro system installed on a river with low head and discharge. The system was assessed under no-load and varying load conditions (25–100%). The results indicate that the generator performs according to the initial design, despite some fluctuations in output parameters. Under no-load conditions, the generator maintains a stable output voltage between 12–14 VAC, with a rotational speed of 590–600 RPM, a system frequency of 59–60 Hz, and zero current. The step-up transformer successfully raises the voltage to 220–222 V with high stability, although minor ripple is observed in the output signal. Under load, the generator voltage slightly decreases to 12–14 V as the load increases. The rotational speed also declines (560–590 RPM), affecting frequency stability, which drops from 59 Hz at 25% load to 56 Hz at full load. The current rises proportionally with the load, from 0.10 A at 25% to 0.45 A at 100%. The observed performance drop under load highlights the effect of load on generator speed and overall system output. The primary impacts of the 25–100% load range are evident in generator speed, frequency stability, and waveform quality. Overall, the system performs satisfactorily for low-head pico-hydro applications with a power capacity of up to 100 Watts, suitable for rural street lighting.

Keywords*: generator, pico-hydro, performance, transformer, voltage.*

I. INTRODUCTION

ACHIEVING global net-zero CO_2 emissions is critical to meeting the Paris Agreement's temperature targets, requiring substantial technological advancements and the removal of barriers in key emitting sectors [1]. There is a growing consensus on the urgent need for global action to limit warming to below 2°C [2]. Indonesia's Nationally Determined Contribution (NDC) reflects its commitment to climate change mitigation, targeting a 29% reduction in greenhouse gas (GHG) emissions by 2030 compared to Business as Usual (BAU) levels [3]. This target significantly relies on the Land Use, Land Use Change, and Forestry (LULUCF) sector for emissions reduction [4].

To meet these goals, it is essential to reduce reliance on carbon-intensive systems by promoting renewable energy. In Spain, gravity water vortex power plants (GWVPP) have proven effective in low-pressure environments by optimizing vortex formation and water velocity, enhancing energy conversion in small hydropower systems [5]. In Laos, while the Namche 1 hydropower plant supports economic development, its environmental and social impacts are considerable, requiring a thorough cost-benefit analysis [6]. In Lithuania, although hydropower plants provide renewable energy, small-scale systems can disrupt river ecosystems, affecting water quality, benthic macroinvertebrate populations, and fish abundance [7]. In the Philippines, hydropower development depends on upstream flow conditions, but

other risks related to surface processes and environmental factors must also be considered. Identifying suitable sites for small-scale hydropower systems involves analyzing landscape dynamics [8].

Indonesia has implemented several renewable energy initiatives, including solar power plants with a capacity of 17.22 MW, geothermal plants at 2,130.7 MW, biomass at 2,200 MW, and hydroelectric plants with an installed capacity of 6,283.3 MW [9]. In one Indonesian project, the optimal setup included 48 units of 600 Wp photovoltaic panels, 17 units of 250 Ah batteries, and 3 units of 8,000 W inverters [10]. Given Indonesia's archipelagic geography and substantial water resources—including seas, major rivers, and small rivers—there is significant potential for hydropower. However, when utilizing small rivers, a permanent countercurrent recirculation vortex in crossflow turbines can lead to turbulence and efficiency loss, which may be mitigated through blade modification [11].

However, carbon emissions continue to arise primarily from the use of generators in various regions of Indonesia. Due to economic considerations and operational reliability, generators remain the preferred option for small and medium-sized businesses such as retail stores, offices, and banks [12]. This study focuses on efforts to reduce carbon emissions in rural and suburban areas. One proposed solution is the use of renewable energy sources, particularly water energy, which holds significant potential for delivering clean and sustainable electricity. In rural areas with unique topographical features, such as lowland contours (low head), harnessing water energy becomes more challenging. Traditional pico-hydro systems in these lowland areas often suffer from limitations in efficiency and power output. This situation necessitates innovation in pico-hydro technology to enable more efficient electricity generation, especially on a scale suitable for rural settings. For instance, a dam fitted with a sluice gate and a trash screen, combined with a waterwheel of 1–3 meters in height and a discharge rate of 0.03 m^3/s, can achieve high efficiency when paired with a propeller water turbine [12], [13], [14], [15]. The potential for pico-hydro use in Indonesia is estimated at 269.52 MW and 43.79 MW, respectively [16]. Effective water management is essential for the conservation, utilization, and regulation of water power. In such systems, electricity is generated through the mechanical rotation of turbines driven by water flow [17], [18]. This study designs a 100 W full-load capacity pico-hydro power plant intended to supply electricity for rural street lighting.

This study offers a novel contribution to the design and implementation of low-head pico-hydro systems by focusing on three key aspects. First, it introduces a portable design adaptable to local river currents, allowing the system to be quickly installed and dismantled at the point of strongest flow—unlike conventional systems, which are typically permanent and less flexible. Second, it utilizes an axial generator based on a used motorcycle spool, modifying the motor spool to optimize the use of local materials. This approach reduces production costs while maintaining high energy conversion efficiency at low rotational speeds, which suits low-head conditions. Third, it provides a detailed performance evaluation under varying real-world load conditions (25%–100%), including analyses of voltage, current, frequency, and voltage transformation efficiency using a step-up transformer for rural street lighting applications. Compared to prior studies, this approach addresses a gap in the development of cost-effective, adaptable, and locally sourced pico-hydro systems and offers comprehensive field test data, which remain limited in similar campus- or rural-based research.

II. Research Method

This section outlines the complete preparation process from initiation to the final construction of the system. It describes the sequential development stages, including preliminary assessment, material selection, component fabrication, and assembly procedures, to ensure system integrity and operational efficiency.

A. Site Selection

This study was conducted at the Brantas Joyo River in Malang City, located at geographical coordinates 7°56'30"N, 112°35'59"E, as shown in Figure 1. The site was selected due to its stable water level of 0.63 m, which provides a consistent water discharge. The river's flow is used to rotate the generator by converting potential energy into mechanical energy, which is then transformed into electrical energy. The availability and consistency of water discharge are critical in determining the system's power output, making this site suitable for implementing pico-hydro technology.

TABLE 1
RIVER DATA COLLECTION

Parameter	Brantas River
Water speed (m/s)	20
River width (m)	8.05
River length (m)	10
Head height (m)	0.53
Water depth (m)	0.50
Water flow rate (m^3/s)	2.0125

Figure 1. Research Location

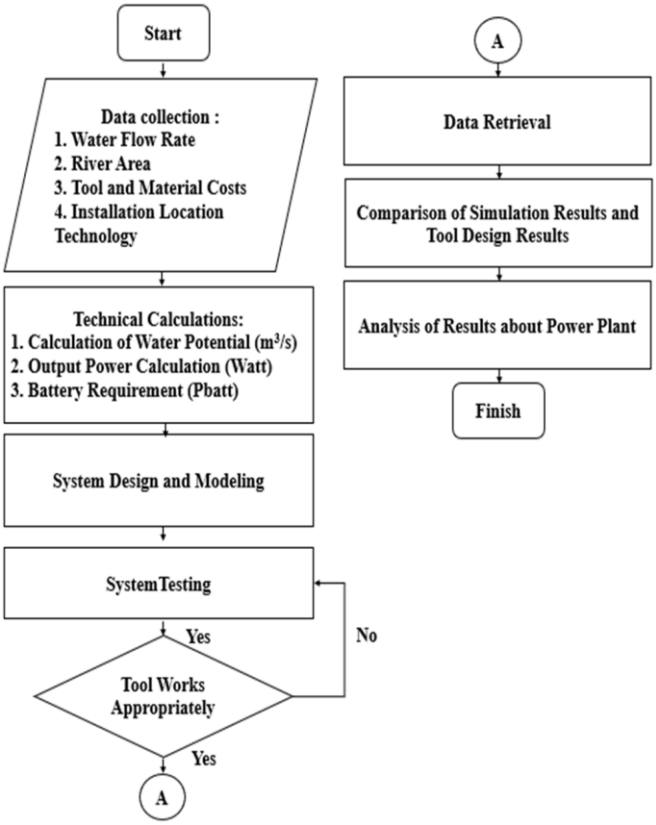

Figure 2. Pico-hydro flowchart

Based on Figure 1 and Table 1, data collection was conducted over four days and recorded periodically. Daily averages were used in the analysis. Based on Table 1, the collected data were used for further calculations using Equation (1). For the Brantas River, the estimated power output is 2 kW. In comparison, three rivers with the same head of 0.53 m were also assessed, and the Joyo Grand River showed a potential pico-hydro power output of 9.4 kW.

B. System Design

The study involved several sequential stages, each designed to optimize power generation. These stages are illustrated in the flowchart in Figure 2. As shown in Figure 2, the primary data collected

TABLE 2
GENERATOR PARAMETERS

Generator Parameter	Specification
Max Gen Voltage (V)	48
Max Current Gen (I)	5
Generator Efficiency (%)	0
System Voltage (V)	12
Temperature (°C)	80

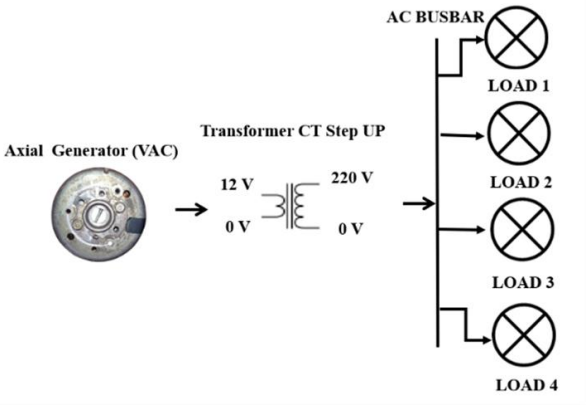

Figure 3. System diagram of low-head pico-hydro

$$\frac{N_p}{N_s} + \frac{V_p}{V_s} \tag{1}$$

included water discharge, river dimensions, equipment costs, and installation site characteristics. Technical calculations were performed to determine water discharge, target power output, and battery requirements. Simulations and modeling were used to define the electrical circuitry and system design. If error margins exceeded 10%, revisions were made before advancing. The system was then assembled according to the simulation results, and periodic data collection was conducted to monitor system performance. Finally, simulation and design outcomes were compared to assess system reliability, compliance, and actual power output.

1) Axial generators

Axial generators in low-flow pico-hydro systems are supported by several components that enable the production of electrical energy with significant output power [21], [22], [23]. In this system, the axial generator serves as the core component, specifically designed to achieve a power capacity of up to 100 Watts. Its working principle is based on the conversion of mechanical energy into electrical energy through electromagnetic induction. The technical specifications of the axial generator used in this study are provided in Table 2.

The charge controller regulates the voltage output from the generator, which is first converted from three-phase Alternating Current (AC) to Direct Current (DC). The controller manages this voltage to identify the optimal operating point, thereby stabilizing the voltage and current produced.

The center-tapped transformer in this system also operates on the principle of electromagnetic induction, similar to conventional transformers. The alternating current (AC) in the primary winding generates a magnetic field in the transformer core, which induces an electromotive force (EMF) in the secondary winding. In the center-tapped configuration, the total voltage in the secondary winding is split into two equal voltages, one on each side of the center tap.

This system also aims to increase water discharge through strategic damming in a controlled turbulent flow environment. The design is optimized to improve flow dynamics and enhance energy capture in low-head conditions, as shown in Figure 3.

2) CT Step-Up Transformer

The CT step-up transformer operates based on the principle of electromagnetic induction, similar to conventional transformers. When alternating current (AC) flows through the primary winding, it generates a magnetic field in the transformer core, which in turn induces an electromotive force (EMF) in the secondary winding. In a center-tapped configuration, the total voltage in the secondary winding is divided into two equal half-voltages, each located on either side of the center tap. In (1), *Np* represents the

TABLE 3
CT STEP-UP TRANSFORMER PARAMETERS

Transformer CT Parameter	Specification
Input Voltage (V_{in})	12-36 VAC
Output Voltage (V_{out})	110-220 VAC
Maximum Current (I_{max})	5 A
Maximum Power (P_{max})	2200 Watt

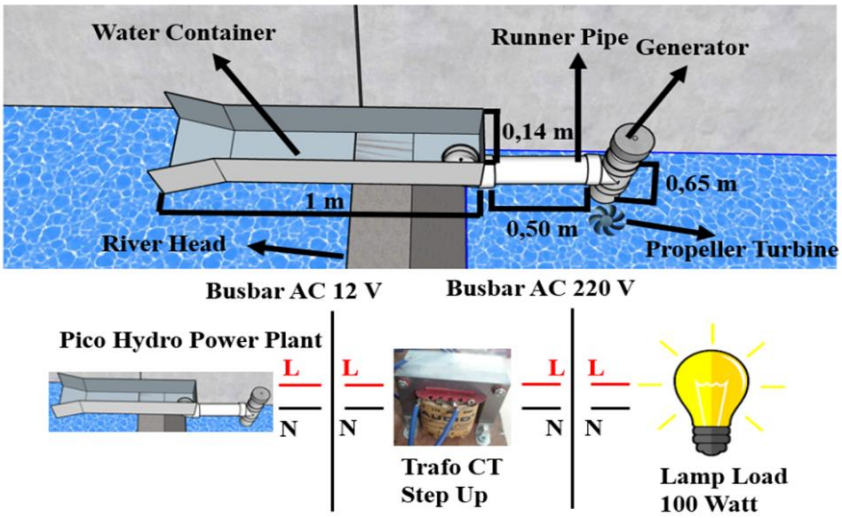

Figure 4. System diagram

number of primary winding turns, N_s the number of secondary winding turns, V_p the primary voltage, and V_s the secondary voltage.

Center-tapped transformers are equipped with a connection at the midpoint of the secondary winding—known as the center tap—which divides the winding into two equal parts. This allows the transformer to deliver two equal but oppositely polarized voltage outputs. As a result, center-tapped transformers are commonly used in full-wave rectifier circuits and other applications requiring both positive and negative voltage outputs. The specifications of the step-up transformer used in this system are presented in Table 3.

C. Simulation and Modeling

To achieve the desired performance targets, an appropriate system design and optimization process are required. The development involves careful evaluation of various parameters and constraints to ensure optimal functionality. This includes systematic analysis of component specifications, material properties, and operational conditions to determine the most effective configuration. Optimization techniques are applied to balance efficiency, cost, and sustainability. Additionally, iterative testing and refinement are conducted to validate the design against defined performance metrics and to resolve any limitations encountered during implementation. This comprehensive approach ensures the final system meets technical requirements while maximizing resource efficiency.

Low-head pico-hydro systems possess specific characteristics that require detailed analysis, particularly in this study, which focuses on axial generators and propeller turbines. Accurate analysis is crucial to ensure the system operates efficiently.

As illustrated in Figure 4, the system comprises several main components, including a generator, propeller turbine, and CT step-up transformer, all tailored to comply with Indonesian electrical load standards [19]. Once the voltage is stepped up to 220 VAC, it can be supplied to the designated load [20]. The system is intended to power public street lighting in the Joyo Grand River area. This application is based on a portable pico-hydro system that can be installed and dismantled as needed, depending on the location of the river's fastest current. The design allows for flexible placement at optimal flow points to maximize energy generation efficiency under local environmental conditions.

1) Potential Low Head River Water Discharge

In developing this pico-hydro power generation system, the lower reaches of the river are utilized as the primary site [25]. The underlying principle is that the greater the water fall (head), the more potential

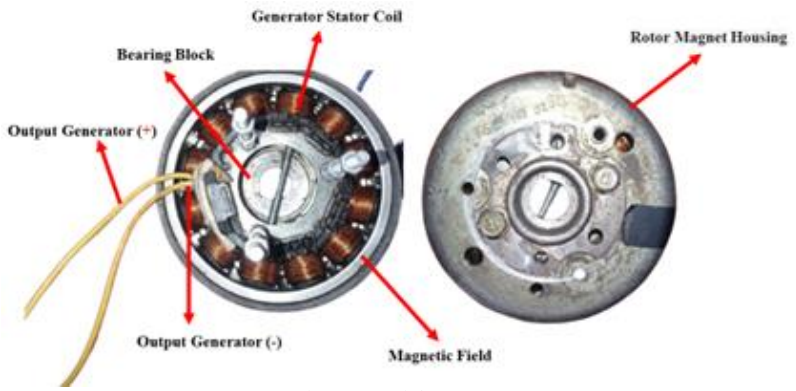

Figure 4. Axial generator

$$Q = A \times v$$
$$Q = (y \times h) \times (x/t) \quad (2)$$

$$P_t = Q \times \rho_{water} \times g \times H \times \eta T \quad (3)$$

$$E_0 = \sqrt{2\pi} \times f \times N_{turn} \times K_w \, x \, r \times q \times \Phi_m \quad (4)$$

$$B_{max} = B_r + I_m / (I_m + \delta) \quad (5)$$

$$A_m = \pi({r_0}^2 + {r_1}^2) - \tau_f \, (r_0 - r_1) \, N_m / N_m \quad (6)$$

energy is available for conversion into electrical energy. To calculate the potential electrical energy generated from water flow, (2) is used, which determines water discharge based on the cross-sectional area and flow velocity.

In (2), Q denotes the water discharge (m^3/s), A is the cross-sectional area of the river (m^2), and v is the water velocity (m/s). The formula can also be expressed in terms of river dimensions, where y is the river width (m), h is the water depth (m), x is the length of water flow (m), and t is time (s). The potential energy available due to water elevation (head) is a crucial factor in estimating the power that can be produced. This theoretical framework underpins pico-hydro systems, which rely on converting the gravitational potential energy of falling water into electricity [27], [25].

2) Generating Power of Water Potential

Water potential energy refers to the energy harnessed from falling water at a given height [26]. This energy must be carefully considered when estimating the power and capacity that can be generated from available water discharge. In this study, a propeller-type turbine operating at a low head and inclined at 30 degrees is used. The water discharge plays a key role in determining the pressure applied to the turbine blades [27]. To calculate the potential electrical power generated from the water flow, (3) is applied.

In (3), P_t represents the potential electrical power output (Watts), Q is the water flow rate (m^3/s), ρ_{water} is the density of water, typically 1000 kg/m^3, g is the acceleration due to gravity (9.81 m/s^2), H is the height of the water fall (head) in meters, and ηT is the efficiency of the turbine, expressed either as a decimal or percentage.

3) Generating Potential Design

The electromotive force (EMF) generated in the stator coil is alternating and rotates synchronously with the speed of the rotor [28]. This EMF results from the variation in magnetic flux intersecting the stator conductor as the rotor turns. To estimate the expected output voltage, the induced voltage equation for generators is used [29], [30]. This equation is essential for designing an efficient generation system and ensuring that the electrical output meets the requirements of the connected load. The generator serves as the core component in converting mechanical energy—derived from the rotation of a waterwheel—into electrical energy. As water flows and drives the waterwheel blades, the resulting rotation turns the generator rotor, producing a magnetic field that induces voltage in the stator coil [13]. The

generator design used in this study is shown in Figure 4. It has been adapted to match the power requirements and rotational speed produced by the waterwheel-based system.

The EMF induced in the stator coil is alternating and synchronized with the rotor's rotational speed [17]. In this design, a used motorcycle spool is repurposed by rewinding the coil to produce the desired voltage output. References [30] and [31] provide formulas for calculating the expected voltage. This method efficiently reuses the existing motor spool structure while tailoring the coil windings to meet specific voltage targets. Equation (4) is used to calculate the output voltage E_0 of a single-phase generator with a radial configuration. This voltage represents the peak EMF induced in the stator coil as a result of the rotating magnetic field.

In (4), f denotes the electrical frequency in Hertz (Hz), N_{turn} is the number of turns in the coil, K_w is the winding factor accounting for coil distribution and arrangement, r is the number of coil layers, q is the number of coils, and Φm is the magnetic flux per pole measured in Weber (Wb). In (4), the variables are defined as follows: f is the frequency in Hertz (Hz), N_{turn} is the number of wire turns, K_w is the winding factor (assumed to be 1), r is the number of layers per coil, q is the number of coils, and Φ_m is the magnetic flux in Weber (W_b). This equation is used to calculate the output voltage for the design of a single-phase radial generator. To determine the strength of the magnet, (5) is applied [31].

In (5), B_{max} is the maximum magnetic flux density (Tesla, T), B_r is the residual flux density (T), I_m is the height of the magnet (m), and δ is the air gap width (m) [32]. The area of the magnet can be calculated using (6). In (6), A_m is the area of the magnet (m^2), r_0 is the outer radius of the magnet (m), r_1 is the inner radius (m), tf is the magnetic distance (m), and N_m is the number of magnets. Finally, to calculate the maximum magnetic flux, (7) is used [32]. In (7), θ_{max} represents the maximum magnetic flux (Wb), A_{magnet} is the area of the magnet (m^2), and B_{max} is the maximum magnetic flux density (T).

D. Assembly and Testing

After the design and simulation stages were completed, the pico-hydro system was assembled using components tailored to the characteristics of the river flow. The assembly process began with the fabrication of a propeller-type turbine mounted on a pipe runner, followed by the installation of an axial generator modified from a used motorcycle spool. The coil was rewound to meet the system's voltage and current requirements. A CT step-up transformer was also integrated to raise the generator's output voltage from 12–14 VAC to the standard 220 VAC, in accordance with the requirements for street lighting.

The complete system was installed at the test site on the Brantas River in Joyo Grand, Malang. This location was selected based on the highest water flow velocity to maximize kinetic energy conversion. A modular installation method was employed, allowing for easy disassembly and reassembly.

Testing was conducted in stages across five load conditions: no load (0%) and incremental loads of 25%, 50%, 75%, and 100% of the system's maximum capacity of 100 Watts. Each load condition was simulated using combinations of 25-Watt lamps, representing typical field applications. For every load variation, output voltage, current, frequency, and generator rotational speed (RPM) were measured using a digital multimeter and a manual tachometer. The data were collected periodically and used to evaluate system stability and verify the results of prior simulations. This testing process is essential to confirm that the system can operate reliably under real-world conditions with varying loads.

E. Validation

System validation was conducted by comparing the simulation results from the design stage with direct field measurements. The validated parameters included generator output voltage, current, frequency, and rotational speed (RPM). Theoretical values were derived using standard formulas for water potential energy and electromagnetic induction, and then compared to actual data obtained from tests under five different load conditions.

All measurements were taken using calibrated digital instruments, with an accuracy of ±0.05 V for voltage, ±0.01 A for current, and ±10 RPM for rotational speed. Frequency was calculated based on the number of magnetic poles in the generator and the observed RPM. The validation results indicated that the deviation between simulation outputs and field measurements remained within acceptable technical tolerance limits. For instance, the simulated no-load output voltage of 13.8 VAC matched the actual measured range of 12–14 VAC. Likewise, the observed frequency decline from 59 Hz to 56 Hz at full load was consistent with the predicted RPM decrease in the design.

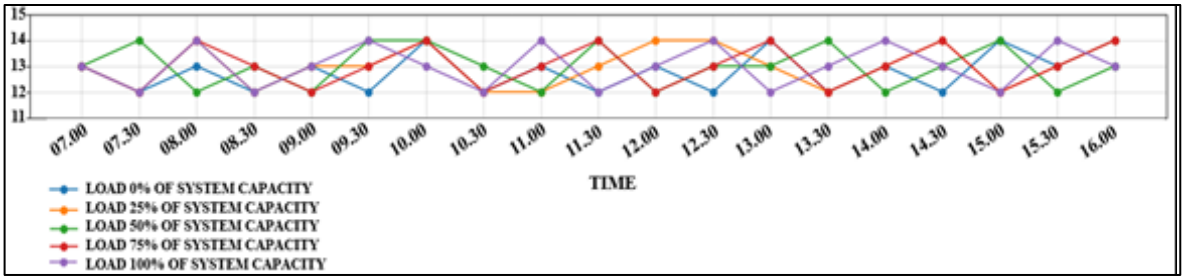

Figure 5. Generator output voltage under 5 load variations

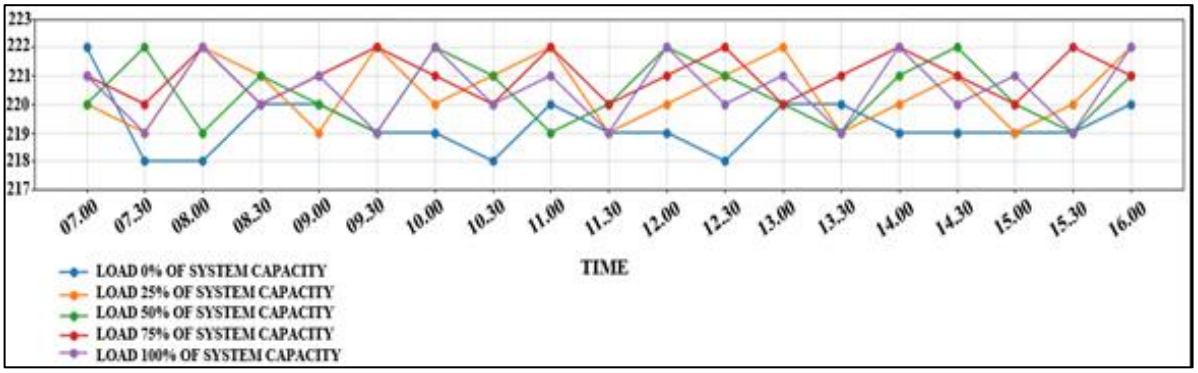

Figure 6. Step-up transformer voltage output under 5 load variations

Overall, the validation process confirmed that the design model and simulation approach offer good accuracy and reliability for implementing small-scale pico-hydro systems in real-world environments. To enhance future accuracy, the integration of automated monitoring systems using data loggers or Internet of Things (IoT) technology is recommended to enable real-time data collection and strengthen system performance evaluation.

III. Results and Discussion

A. Analysis of Runner Pipe Pico-Hydro

In this study, a low-head pico-hydro system was designed to utilize the pressure generated by falling water. The objective is to drive the water turbine to rotate at high speed. The system was developed using Bernoulli's principle and the law of fluid continuity. When water enters the runner pipe with a diameter of 0.9 m, the discharge measured in Runner 1 (horizontal orientation) is 0.0063585 m^3/s, while Runner 2 (vertical orientation) records a discharge of 0.0041330 m^3/s.

B. Analysis of Axial Generator Pico-Hydro

The pico-hydro system is designed to supply electrical power up to 100 Watts, requiring a stable and reliable power source. To achieve the target voltage, appropriate winding calculations and mechanical design adjustments are essential. In this case, the magnetic flux density was measured at 0.0000714285714285714 T, with a cross-sectional area Am of 0.858 m^2, resulting in a maximum magnetic flux of approximately 0.0000613 Wb. The frequency, determined by the generator's rotational speed and the number of magnetic poles, is calculated to be 60 Hz. Based on these parameters, the resulting electromotive force (EMF) generated is approximately 13.8 V.

C. Generator Voltage Output Results – 5 Load Variations

The test results for generator voltage output under five different load conditions are presented in Figure 5. Based on the test results shown in Figure 5, the generator's output voltage under no-load conditions ranges from 12 to 14 VAC. This output is consistent with the system design, which targets a nominal voltage of 12 VAC, aligning with the available head and relatively low water discharge. Both theoretical calculations and actual test results confirm a matching output of 13.8 VAC, indicating the accuracy of the design. The pico-hydro system was designed to deliver a total power output of 100 Watts. During testing with a 25% load (using a 25-Watt lamp), the generator maintained an output voltage between 13 and 14 V. This result reflects the relatively high rotational speed of the generator under light load. However, when tested with higher loads—50%, 75%, and 100% of capacity—corresponding to 2, 3, and 4

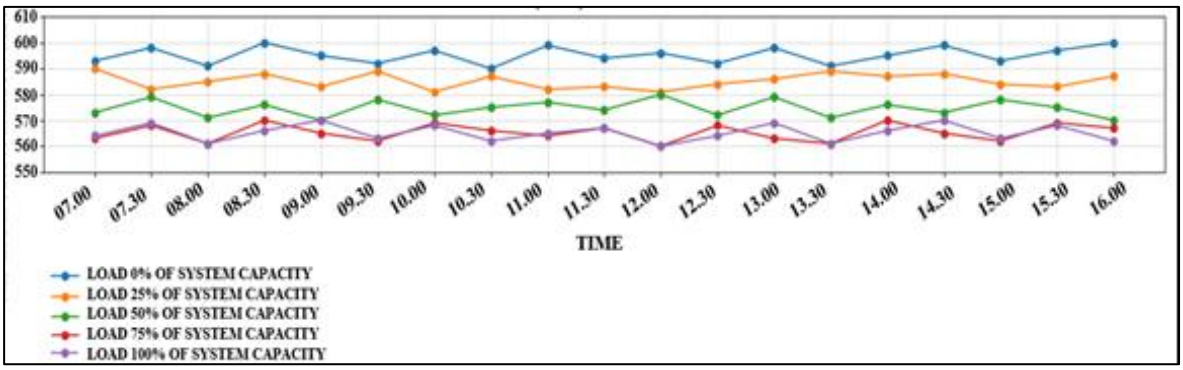

Figure 7 Effect of generator rotational speed (RPM) on output voltage under 5 load variations

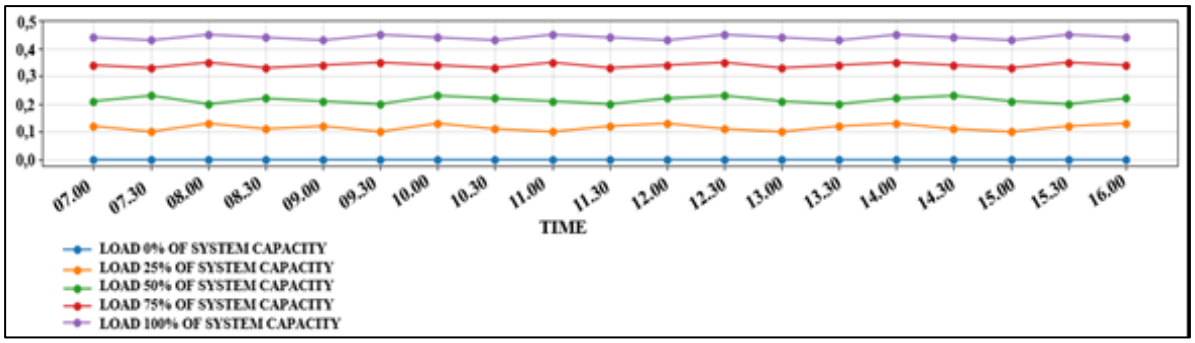

Figure 8. Electric current output under 5 load variations

units of 25-Watt lamps respectively, the generator voltage slightly decreased to a range of 12–13 V. This voltage drop is attributed to the increased load, which causes a reduction in generator rotational speed.

D. CT Step-Up Transformer Voltage Results – 5 Load Variations

To evaluate the performance of the CT step-up transformer, voltage output under each load condition was measured. The results are presented in the table below Figure 6. As shown in Figure 6, a CT step-up transformer is used to raise the generator output to 220 V, in accordance with the Indonesian standard voltage. The transformer output ranges between 218–222 V, indicating a relatively stable voltage under both no-load and loaded conditions. The step-up process uses a winding ratio of Np:Ns=1:18N_p : N_s = 1 : 18, producing an output voltage within ±1% of the nominal 220 V. The voltage output varies slightly depending on the applied load. At 25% load, the transformer output is typically in the range of 220–222 V. As the load increases to 50%, the voltage stabilizes within 220–221 V. Under a 75% load, the voltage output generally falls between 219–220 V. When the load is reduced back to 25%, the voltage remains steady in the 219–220 V range. These minor fluctuations are attributed to changes in generator rotational speed, which affect the input voltage to the transformer and subsequently influence the output voltage. This relationship highlights the dependency between generator speed and voltage stability in the step-up process.

E. Output Results of Generator Rotation (Nrev) with 5 Load Variations

To assess the step-up transformer's voltage output, an analysis of the test results was conducted, as illustrated in Figure 8. The figure highlights the voltage increase achieved by the system, showing the relationship between the input and output voltages. The data demonstrates the transformer's efficiency in converting low input voltage into a higher output voltage, confirming its effectiveness for electrical applications.

Based on the test results presented in Figure 7, the generator's rotational speed—driven by the river's flow—ranges from 590 to 600 RPM, which aligns with the system design expectations. This relatively low rotational speed confirms the suitability of the axial generator, which uses permanent magnets to produce voltage efficiently at low RPM. The generator, built using a repurposed motorcycle spool, operates with an estimated efficiency of around 60%. Under a 25% load, the generator's RPM falls slightly to a range of 580–590. As the load increases to 50%, the RPM drops further to 570–580. At 75% and 100% load, the rotational speed stabilizes in the 560–570 RPM range. These reductions in RPM with

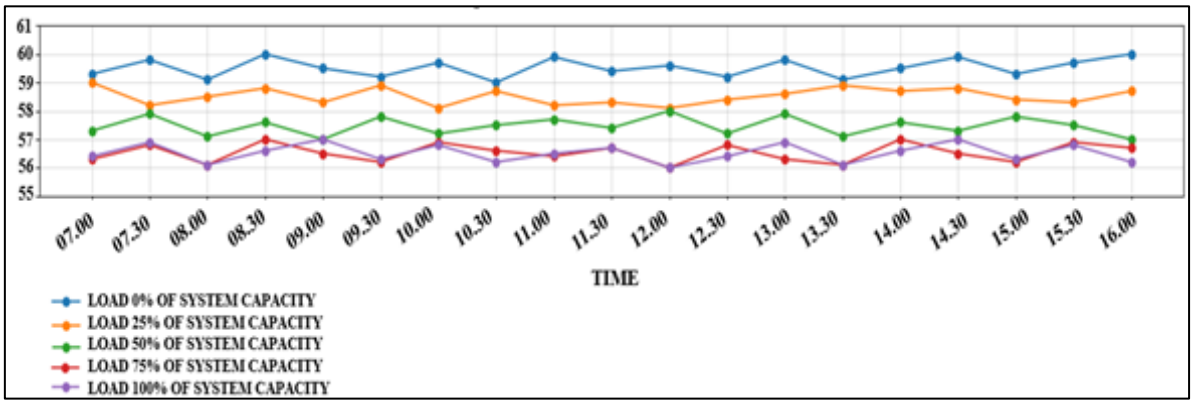

Figure 9. Generator output frequency under 5 load variations

increased load directly affect the electrical output, particularly the current. The current generated is influenced by the coil design, which in this case uses copper wire with a diameter of 0.8 mm.

F. Generator Current Results with 5 Load Variations

By analyzing the data presented in Figure 7, the generator's efficiency, operational stability, and ability to supply current under real-world conditions can be evaluated. The results of the current output during testing are shown in Figure 8.

Based on the system testing shown in Figure 8, the generator was designed to deliver a maximum output of 100 Watts. In the initial test without load, the axial generator—rewound using 0.8 mm copper wire, with 12 turns and 6 stacked layers—produced a current of 0 A. This result is expected, as no electrical load was applied to the system. When a 25% load was applied, the generated current ranged from 0.10 to 0.13 A. At 50% load, the current increased to approximately 0.20–0.23 A. Under a 75% load, the system produced a current in the range of 0.33–0.35 A. Finally, at full load (100%), the current output reached 0.43–0.45 A. These results clearly demonstrate a direct relationship between the load applied and the current generated. As the load increases, the system must supply a proportionally higher current to maintain stable operation and meet energy demands. This relationship highlights the importance of designing the system to accommodate varying load conditions, ensuring that sufficient current can be generated without compromising performance or reliability.

G. Frequency Results with 5 Load Variations

To analyze the system frequency under load conditions ranging from 25% to 100%, a detailed evaluation was conducted. The results are presented in Figure 9, which illustrates how the system's frequency responds to varying load levels. This analysis provides insight into the operational stability and performance of the system. By examining the data, the system's ability to maintain a consistent frequency under increasing load can be assessed—an essential factor in ensuring reliable energy generation and delivery.

As shown in Figure 9, the system operates at a frequency of approximately 59–60 Hz under no-load conditions. The output frequency is influenced by the generator's rotational speed (RPM), with higher RPM values resulting in higher frequencies. In this design, the generator features 12 magnetic poles, which determine the output frequency through the established relationship between RPM and the number of poles. Consequently, changes in rotational speed directly affect the frequency stability of the system.

When compared to other pico-hydro implementations, such as those reported in [15] and [18], the system developed in this study demonstrates stable performance under low-head conditions, achieving an energy conversion efficiency of approximately 60%. This is notable given the use of recycled components, such as repurposed motorcycle coils. Prior studies using specialized components have reported typical efficiencies ranging from 55% to 65%, positioning the current design as competitive both in performance and cost-effectiveness.

Further comparisons with systems developed by [41] and [42] support these findings. For instance, Gallego et al. reported efficiencies of around 55–65% using commercial components, whereas the pre-

sent system achieves comparable performance using locally sourced and recycled materials. This highlights the potential for low-cost, community-fabricated pico-hydro systems to deliver reliable and efficient energy under real-world, low-head conditions.

In terms of voltage stability, the system consistently maintained 12–14 VAC before the step-up process and 218–222 VAC after step-up across varying load conditions. These results are comparable to the typical output levels of micro-hydro systems used in rural applications, as reported by [43]. The system also demonstrated acceptable frequency stability, ranging from 59 Hz at no load to 56 Hz under full load—performance similar to Turgo turbine-based systems referenced in prior studies.

H. Current System Limitations

Despite its promising performance, the system exhibits several limitations that must be addressed for practical, long-term implementation. Under maximum load conditions, significant drops in frequency and RPM were observed, indicating sensitivity to overloading. This underscores the need for mechanical reinforcement and the incorporation of adaptive load control mechanisms to enhance reliability. Additionally, the current design lacks proper weatherproofing, making critical components vulnerable to environmental factors such as rain and humidity. Future versions should include IP-rated enclosures to improve durability under outdoor conditions. Another major limitation is the absence of energy storage; the system operates entirely on a direct load basis. Incorporating energy storage solutions—such as battery banks or supercapacitor modules—would allow for greater power stability and overall system resilience.

All voltage and current measurements were conducted using a calibrated digital multimeter with accuracy levels of ±0.05 V and ±0.01 A, respectively [44]. Generator RPM was estimated based on rotor speed, with an error margin of approximately ±10 RPM. Frequency was calculated using the standard formula involving pole count and RPM, with expected deviations within ±1 Hz [45].

Although these margins are relatively small, system accuracy and monitoring could be significantly improved through the use of real-time data loggers and automated monitoring systems in future implementations [46].

Although the system demonstrated promising performance, several limitations must be acknowledged. Under full-load conditions, a noticeable drop in frequency and rotational speed (RPM) was observed, indicating the need for improved load management and mechanical reinforcement. Additionally, the current design lacks environmental protection, making components susceptible to rain and high humidity due to the absence of a waterproof enclosure. To address these issues, future designs should incorporate key enhancements. These include the integration of IP-rated protection for electrical components, mechanical improvements to maintain stable generator speed under heavy loads, and the addition of energy storage systems such as batteries or supercapacitors to enhance power stability. Furthermore, the implementation of a smart control system based on Internet of Things (IoT) technology is recommended to enable dynamic load management and optimize operational efficiency.

I. Measurement Uncertainty and Error Margins

Voltage and current measurements were conducted using a calibrated digital multimeter, with uncertainties of ±0.05 V and ±0.01 A, respectively. The estimated generator rotational speed had an error margin of ±10 RPM. Although these margins are relatively small, incorporating an automated monitoring system in future studies is recommended to enable real-time data validation and improve measurement accuracy.

IV. CONCLUSION

Based on the test results under no-load and 25–100% load conditions, the pico-hydro system demonstrated performance consistent with the initial design, despite some variations in output parameters. Under no-load conditions, the generator output voltage remained stable between 12–14 VAC, with a rotational speed of 590–600 RPM, a system frequency of 59–60 Hz, and zero current. The step-up transformer successfully increased the voltage to 220–222 V with high stability, although slight ripple was observed in the output signal. Under load conditions (25–100%), the generator output voltage slightly decreased to 12–14 V as the load increased. The rotational speed dropped to 560–590 RPM, resulting in a frequency decrease from 59 Hz at 25% load to 56 Hz at full load. The current increased proportionally with the load, ranging from 0.10 A at 25% to 0.45 A at 100%. These results indicate that load

variations affect generator rotation, frequency stability, and waveform quality. As the load increases, the generator's rotational speed declines due to increased mechanical resistance, impacting overall system output. Overall, the system performs reliably and efficiently for pico-hydro applications with power capacities of up to 100 Watts, making it a viable solution for rural and low-head energy generation needs.

ACKNOWLEDGMENT

This research was supported by Non-APBN UM 2024, Indonesia, under contract number 11.6.53/UN32.14.1/LT/2024.

REFERENCES

[1] P. Gabrielli *et al.*, "Net-zero emissions chemical industry in a world of limited resources," Jun. 16, 2023, *Cell Press*. doi: 10.1016/j.oneear.2023.05.006.

[2] R. S. Haszeldine, S. Flude, G. Johnson, and V. Scott, "Negative emissions technologies and carbon capture and storage to achieve the Paris Agreement commitments," May 13, 2018, *Royal Society Publishing*. doi: 10.1098/rsta.2016.0447.

[3] J. Rogelj, "Net zero targets in science and policy," *Environmental Research Letters*, vol. 18, no. 2, Feb. 2023, doi: 10.1088/1748-9326/acb4ae.

[4] Y. Kaya, M. Yamaguchi, and O. Geden, "Towards net zero CO2 emissions without relying on massive carbon dioxide removal," Nov. 01, 2019, *Springer Tokyo*. doi: 10.1007/s11625-019-00680-1.

[5] Y. Jiang *et al.*, "Multi–Disciplinary Optimizations of Small-Scale Gravitational Vortex Hydropower (SGVHP) System through Computational Hydrodynamic and Hydro–Structural Analyses," *Sustainability (Switzerland)*, vol. 14, no. 2, Jan. 2022, doi: 10.3390/su14020727.

[6] M. M. Rahman, J. H. Tan, M. T. Fadzlita, and A. R. Wan Khairul Muzammil, "A Review on the Development of Gravitational Water Vortex Power Plant as Alternative Renewable Energy Resources," in *IOP Conference Series: Materials Science and Engineering*, Institute of Physics Publishing, Jul. 2017. doi: 10.1088/1757-899X/217/1/012007.

[7] D. Vasile Banyai, I. Radu Pop, D. Opruta, And L. Ioan Vaida, "Acta Technica Napocensis Series: Applied Mathematics Optimal Flow Control For Increased Electricity Production In Small Hydropower Plants," 2018.

[8] I. Torrefranca, R. E. Otadoy, and A. Tongco, "Incorporating Landscape Dynamics in Small-Scale Hydropower Site Location Using a GIS and Spatial Analysis Tool: The Case of Bohol, Central Philippines," Energies (Basel), vol. 15, no. 3, p. 1130, Feb. 2022, doi: 10.3390/en15031130.

[9] F. Paundra and A. Nurdin, "Study Of The Potential And Development Of Renewable Energy Power In Indonesia : A Review," Steam Engineering, vol. 3, no. 2, pp. 62–72, Mar. 2022, doi: 10.37304/jptm.v3i2.4024.

[10] Aripriharta, D. A. Putri, A. P. Wibawa, Sujito, M. C. Bagaskoro, and S. Omar, "Techno economic analysis of PV pumping system for rural village in East Java," e-Prime - Advances in Electrical Engineering, Electronics and Energy, vol. 10, p. 100779, Dec. 2024, doi: 10.1016/j.prime.2024.100779.

[11] R. Irwansyah, Warjito, Budiarso, C. Clement Rusli, and S. B. Nasution, "Analysing Hydraulic Efficiency of Water Vortex Pico-Hydro Turbine using Numerical Method," Journal of Advanced Research in Fluid Mechanics and Thermal Sciences, vol. 77, no. 2, pp. 91–101, Nov. 2020, doi: 10.37934/arfmts.77.2.91101.

[12] I. Samora, V. Hasmatuchi, C. Münch-Alligné, M. J. Franca, A. J. Schleiss, and H. M. Ramos, "Energy production with a tubular propeller turbine," IOP Conference Series Earth and Environmental Science, vol. 49, p. 102001, Nov. 2016, doi: 10.1088/1755-1315/49/10/102001.

[13] M. Kiraga, "Hydroelectric Power Plants and River Morphodynamic Processes," Journal of Ecological Engineering, vol. 22, no. 7, pp. 163–178, 2021, doi: 10.12911/22998993/139068.

[14] G. J. Jong, Aripriharta, Hendrick, and G. J. Horng, "A Novel Queen Honey Bee Migration (QHBM) Algorithm for Sink Repositioning in Wireless Sensor Network," Wirel Pers Commun, vol. 95, no. 3, pp. 3209–3232, Aug. 2017, doi: 10.1007/s11277-017-3991-z.

[15] L. C. Alvear Pérez, M. J. Anaya Acosta, and C. A. Pedraza Yepes, "CFD simulation data of a pico-hydro turbine," Data Brief, vol. 33, Dec. 2020, doi: 10.1016/j.dib.2020.106596.

[16] A. Aripriharta, E. Asnarindra, A. D. Nibrosoma, L. Gumilar, and M. A. Habibi, "Pelacakan Daya Maksimum Photovoltaic Dalam Keadaan Transisi Berbayang Menggunakan Algoritma Mppt Queen Honey Bee Migration (QHBM)," Transmisi: Jurnal Ilmiah Teknik Elektro, vol. 25, no. 3, pp. 85–94, Jul. 2023, doi: 10.14710/transmisi.25.3.85-94.

[17] E. Gallego, A. Rubio-Clemente, J. Pineda, L. Velásquez, and E. Chica, "Experimental analysis on the performance of a pico-hydro Turgo turbine," Journal of King Saud University - Engineering Sciences, vol. 33, no. 4, pp. 266–275, May 2021, doi: 10.1016/j.jksues.2020.04.011.

[18] A. Židonis, D. S. Benzon, and G. A. Aggidis, "Development of hydro impulse turbines and new opportunities," Aug. 07, 2015, Elsevier Ltd. doi: 10.1016/j.rser.2015.07.007.

[19] K. Shimokawa, A. Furukawa, K. Okuma, D. Matsushita, and S. Watanabe, "Experimental study on simplification of Darrieus-type hydro turbine with inlet nozzle for extra-low head hydropower utilization," Renew Energy, vol. 41, pp. 376–382, May 2012, doi: 10.1016/j.renene.2011.09.017.

[20] A. Date, A. Date, and A. Akbarzadeh, "Investigating the potential for using a simple water reaction turbine for power production from low head hydro resources," Energy Convers Manag, vol. 66, pp. 257–270, 2013, doi: 10.1016/j.enconman.2012.09.032.

[21] I. Torrefranca, R. E. Otadoy, and A. Tongco, "Incorporating Landscape Dynamics in Small-Scale Hydropower Site Location Using a GIS and Spatial Analysis Tool: The Case of Bohol, Central Philippines," Energies (Basel), vol. 15, no. 3, p. 1130, Feb. 2022, doi: 10.3390/en15031130.

[22] K. Gaiser, P. Erickson, P. Stroeve, and J.-P. Delplanque, "An experimental investigation of design parameters for pico-hydro Turgo turbines using a response surface methodology," Renew Energy, vol. 85, pp. 406–418, Jan. 2016, doi: 10.1016/j.renene.2015.06.049.

[23] S. R. Sheikh et al., "A Low-Cost Sustainable Energy Solution for Pristine Mountain Areas of Developing Countries," Energies (Basel), vol. 14, no. 11, p. 3160, May 2021, doi: 10.3390/en14113160.

[24] E. Akbari and M. S. Shadlu, "A Novel Modified Fuzzy-Predictive Control of Permanent Magnet Synchronous Generator Based Wind Energy Conversion System," Chinese Journal of Electrical Engineering, vol. 9, no. 4, pp. 107–121, Dec. 2023, doi: 10.23919/CJEE.2023.000042.

[25] S. J. Williamson, A. Griffo, Stark. B.H, and Booker. J.D, Control of Parallel Single-Phase Inverters in a Low-Head Pico-Hydro Off-Grid Network. 2013.

[26] D. Mitrovic et al., "Multi-Country Scale Assessment of Available Energy Recovery Potential Using Micro-Hydropower in Drinking, Pressurised Irrigation and Wastewater Networks, Covering Part of the EU," Water (Basel), vol. 13, no. 7, p. 899, Mar. 2021, doi: 10.3390/w13070899.

[27] L. Chang and W. Wei, "Numerical study on the effect of tangential intake on vortex dropshaft assessment using pressure distributions," Engineering Applications of Computational Fluid Mechanics, vol. 16, no. 1, pp. 1100–1110, Dec. 2022, doi: 10.1080/19942060.2022.2072954.

[28] W. Cao, "Comparison of IEEE 112 and new IEC standard 60034-2-1," IEEE Transactions on Energy Conversion, vol. 24, no. 3, pp. 802–808, 2009, doi: 10.1109/TEC.2009.2025321.

[29] A. E. Putra, "Perancangan Dan Pembuatan Generator Fluks Radial Satu Fasa Menggunakan Lilitan Kawat Sepeda Motor Dengan Variasi Diameter Kawat," 2014.

[30] C.-S. Yi, K.-H. Kim, J.-H. Lee, and M.-P. Shim, "Location Analysis for Developing Small Hydropower Using Geo-Spatial Information System," Journal of Korea Water Resources Association, vol. 40, no. 12, pp. 985–994, Dec. 2007, doi: 10.3741/jkwra.2007.40.12.985.

[31] E. Gómez-Llanos, P. Durán-Barroso, J. Arias-Trujillo, J. M. Ceballos-Martínez, J. A. Torrecilla-Pinero, and M. Candel-Pérez, "Small and Micro-Hydropower Plants Location by Using Geographic Information System," MDPI AG, Oct. 2018, p. 1300. doi: 10.3390/proceedings2201300.

[32] R. Ayu Mustikasari and T. Hardianto, "Analisis Generator Sinkron Permanen Magnet (PMSG) Tipe Radial 3 Fasa dengan Hubungan Kumparan Delta."

[33] E. Buchicchio, A. De Angelis, F. Santoni, P. Carbone, F. Bianconi, and F. Smeraldi, "Battery SOC estimation from EIS data based on machine learning and equivalent circuit model," Energy, vol. 283, Nov. 2023, doi: 10.1016/j.energy.2023.128461.

[34] Y. Zhu, Y. Xiong, J. Xiao, T. Yi, C. Li, and Y. Sun, "An improved coulomb counting method based on non-destructive charge and discharge differentiation for the SOC estimation of NCM lithium-ion battery," J Energy Storage, vol. 73, Dec. 2023, doi: 10.1016/j.est.2023.108917.

[35] S. Amini, S. Bahramara, H. Golpîra, B. Francois, and J. Soares, "Techno-Economic Analysis of Renewable-Energy-Based Micro-Grids Considering Incentive Policies," Energies (Basel), vol. 15, no. 21, Nov. 2022, doi: 10.3390/en15218285.

[36] İ. Çetinbaş, B. Tamyürek, and M. Demirtaş, "Design, analysis and optimization of a hybrid microgrid system using HOMER software: Eskişehir osmangazi university example," International Journal of Renewable Energy Development, vol. 8, no. 1, pp. 65–79, Feb. 2019, doi: 10.14710/ijred.8.1.65-79.

[37] A. Günther, J. Gütschow, and M. L. Jeffery, "NDCmitiQ v1.0.0: a tool to quantify and analyse greenhouse gas mitigation targets," Geosci Model Dev, vol. 14, no. 9, pp. 5695–5730, Sep. 2021, doi: 10.5194/gmd-14-5695-2021.

[38] X. Li, Y. Li, H. Zhou, Z. Fu, X. Cheng, and W. Zhang, "Research on the Carbon Emission Baselines for Different Types of Public Buildings in a Northern Cold Areas City of China," Buildings, vol. 13, no. 5, p. 1108, Apr. 2023, doi: 10.3390/buildings13051108.

[39] Ł. Skowron et al., "Interconnection between the Dynamic of Growing Renewable Energy Production and the Level of CO2 Emissions: A Multistage Approach for Modeling," Sustainability, vol. 15, no. 12, p. 9473, Jun. 2023, doi: 10.3390/su15129473.

[40] A. Günther, J. Gütschow, and M. L. Jeffery, "NDCmitiQ v1.0.0: a tool to quantify and analyse greenhouse gas mitigation targets," Geosci Model Dev, vol. 14, no. 9, pp. 5695–5730, Sep. 2021, doi: 10.5194/gmd-14-5695-2021.

[41] E. Gallego, A. Rubio-Clemente, J. Pineda, L. Velásquez, and E. Chica, "Experimental analysis on the performance of a pico-hydro Turgo turbine," Journal of King Saud University - Engineering Sciences, vol. 33, no. 4, pp. 266–275, May 2021, doi: 10.1016/j.jksues.2020.04.011.

[42] [2] A. Židonis, D. S. Benzon, and G. A. Aggidis, "Development of Hydro Impulse Turbines and New Opportunities."

[43] [3] I. Torrefranca, R. E. Otadoy, and A. Tongco, "Incorporating Landscape Dynamics in Small-Scale Hydropower Site Location Using a GIS and Spatial Analysis Tool: The Case of Bohol, Central Philippines," Energies (Basel), vol. 15, no. 3, Feb. 2022, doi: 10.3390/en15031130.

[44] S. J. Williamson, A. Griffo, B. H. Stark, and J. D. Booker, "Control of parallel single-phase inverters in a low-head pico-hydro off-grid network," in IECON 2013 - 39th Annual Conference of the IEEE Industrial Electronics Society, 2013, pp. 1571–1576. doi: 10.1109/IECON.2013.6699367.

[45] S. R. Sheikh et al., "A low-cost sustainable energy solution for pristine mountain areas of developing countries," Energies (Basel), vol. 14, no. 11, Jun. 2021, doi: 10.3390/en14113160.